Title:

Porous Shape Memory Alloys, Part II:
Modeling of the Thermomechanical Response

Authors:

Pavlin B. Entchev
Dimitris C. Lagoudas
Muhammad A. Qidwai
Virginia G. DeGiorgi

20020715 103

ABSTRACT

Shape memory alloys (SMAs) have emerged as a class of materials with unique thermal and mechanical properties that have found numerous applications in various engineering areas. There have been a variety of applications that perform in a quasi-static manner. Recent work has proposed the use of porous SMAs as an energy absorbing material under dynamic loading conditions. Porous SMAs hold the promise of making high-efficiency damping devices that are superior to those made of conventional materials. The focus of this work is on establishing the quasi-static properties of porous SMA material. To accomplish this, a micromechanics-based analysis of the overall behavior of porous SMA is carried out. The porous SMA is modeled as a composite with SMA matrix, which is modeled using an incremental formulation, and pores as inhomogeneities of zero stiffness. The macroscopic constitutive behavior of the effective medium is established using the incremental Mori-Tanaka averaging method for a random distribution of pores, and a FEM analysis of a unit cell for a periodic arrangement of pores. In addition, a mesoscale level analysis allowing for the examination of pore size and shape variation effects is performed.

Pavlin B. Entchev, Dimitris C. Lagoudas, Aerospace Engineering Department,
    Texas A&M University, College Station, TX 77843-3141.
Muhammad A. Qidwai, Geo-Centers, Inc., PO Box 441340, Fort Washington, MD 20749.
Virginia G. DeGiorgi, Naval Research Laboratory, 4555 Overlook Ave. SW,
    Washington, DC 20375

1. INTRODUCTION

Various applications of porous SMAs have been discussed in Part I of this paper. However, in order to successfully apply porous SMAs in structural applications, their behavior must be well understood under both quasi-static and dynamic loading conditions. An understanding of the static behavior is a basis for continuation of work into the dynamic response regime. Thus the current work focuses on the quasi-static modeling of porous SMAs.

There is a great number of research papers available in the literature devoted to modeling of porous materials. Since the structure of equations representing SMA constitutive behavior can be very similar to those of rate-independent plasticity models, the works dealing with plastic response of porous metals are of particular interest. Here we present a brief overview of some of the representative works.

Different modeling aspects of cellular solids are presented by Gibson and Ashby [1]. The modeling of the mechanical properties in their work is done on the cell level. For the case of open cells it is assumed that each cell is formed by struts, modeled using beam theory. For the case of closed cells, the faces of the cells are modeled as membranes. Both elastic properties and initiation of plasticity are considered. An approach based on unit cell method is presented by Herakovich and Baxter [2]. Their work considers porous material, which possesses a periodic structure such that a repeating representative volume element can be identified. Herakovich and Baxter [2] studied the effect of the pore geometry on the macroscopic response of the porous material for both elastic and elasto-plastic cases.

A different approach based on the mixture theory is presented by Breuer and Jägering [3] for the case of fluid-saturated porous material. Both elastic and elasto-plastic behaviors are considered for the case of incompressible matrix and incompressible fluid. Another approach for modeling plastic behavior of porous solids found in the literature is to derive a macroscopic constitutive law [4-6].

Micromechanical averaging techniques can also be used to determine the averaged macroscopic response. In this case the porous material is treated as a composite with two phases: solid matrix and pores. Different approaches are taken in this work: one approach is to adapt an existing micromechanical averaging scheme to porous SMA behavior; a second approach is based on the unit cell representation of periodic structures; finally, a mesoscale analysis of a representative volume element (RVE) is performed.

There are two widely used averaging methods: the self-consistent method and the Mori-Tanaka method. Both approaches have recently been applied to obtaining effective properties of composites with inelastic phases. For example Lagoudas *et al.* [7] have used an incremental formulation of the Mori-Tanaka method to obtain the effective properties of a composite with elastoplastic matrix and elastic fibers. In a different work, Lagoudas *et al.* [8] have applied the incremental Mori-Tanaka method to model the behavior of a composite with elastic matrix and SMA fibers. Another group of researchers has applied the self-consistent technique to obtain the effective properties of a composite with elastoplastic matrix and SMA

fibers [9]. The method of choice in this work is the Mori-Tanaka method in incremental formulation.

An alternative formulation that assumes periodic arrangement of pores is also used. Both periodicity and symmetry boundary conditions reduce the analysis of the porous SMA material to the analysis of a unit cell [10]. For the mesoscale analysis the representative volume element is chosen based on the assumption that the distribution of pores, their size, shape and volume fraction in it are representative of the overall porous material. Both the unit cell and the mesoscale analyses are carried out using finite element method with the help of an existing dense SMA thermomechanical model [10,11].

The remainder of the paper is organized as follows: Section 2 briefly describes the incremental formulation of the Mori-Tanaka method; Section 3 is devoted to the unit cell FEM, Section 4 describes the mesoscale approach. Section 5 contains results and discussions. Finally some conclusions are made.

2. MORI-TANAKA AVERAGING METHOD

For the application of the Mori-Tanaka averaging method the material is treated as a two-phase composite made of the dense SMA matrix and pores. The modeling of the dense SMA matrix is carried out using an existing rate-independent constitutive model [10,11]. Details of the model can be obtained from these references and are not given here for brevity.

The SMA matrix is characterized by the microscopic stress σ_{ij}^m and strain ε_{ij}^m. Macroscopically the composite is characterized by the stress Σ_{ij} and strain E_{ij}, which are uniform over the RVE and are computed by volume averaging the correspondent microscopic quantities. For simplicity the description is restricted to a two-phase material, i.e., solid SMA matrix and pores of identical shape. Thus the porous SMA is characterized by the pore volume fraction c_p and the pore shape. Assuming isothermal conditions and following the standard micromechanics approach, the relation between the globally applied increment of strain dE_{ij} to the local increment of strain in the matrix $d\varepsilon_{ij}^m$ is:

$$d\varepsilon_{ij}^m(x_n) = A_{ijkl}^m(x_n)dE_{kl},\qquad(1)$$

where $A_{ijkl}^m(x_n)$ is the matrix strain concentration factor and x_n are the components of the position vector. Taking the volume average of Eq.(1) yields:

$$\left\langle d\varepsilon_{ij}^m(x_n)\right\rangle = \left\langle A_{ijkl}^m(x_n)\right\rangle dE_{kl}.\qquad(2)$$

The average matrix strain concentration factor $A_{ijkl}^m = \left\langle A_{ijkl}^m(x_n)\right\rangle$ is found from the following relation:

$$c_p A_{ijkl}^p + (1-c_p)A_{ijkl}^m = \delta_{ijkl},\qquad(3)$$

where A_{ijkl}^p is the average strain concentration for the inhomogeneities (pores), δ_{ijkl} is the fourth order identity tensor. The pore strain concentration factor A_{ijkl}^p is evaluated using the Mori-Tanaka averaging scheme [7]. The algorithm based on the

incremental Mori-Tanaka averaging scheme was implemented in a user subroutine (UMAT) which was complied with the commercial FEM package ABAQUS. The Eshelby tensor, required to compute the concentration factors, cannot be found in closed form for the case of general loading because the phase transformation introduces anisotropy of the tangent stiffness tensors. Therefore, a numerical evaluation of the Eshelby tensor is employed in this work [12].

3. UNIT CELL FINITE ELEMENT METHOD

The unit cell FEM is used for both open-pore and closed-pore material. In-plane hexagonal arrangement of pores is assumed for the case of the open pores [13] and the open pores are assumed to be in the form of circular cylinders with generators in the direction of the out-of-plane axis of the dense SMA matrix. The resultant material possesses transverse isotropy similar to what would have been obtained if the cylinders were randomly arranged. On the other hand, closed pores are spheres distributed in a hexagonal arrangement in a plane cut and in equi-distant layers in the out-of-plane direction.
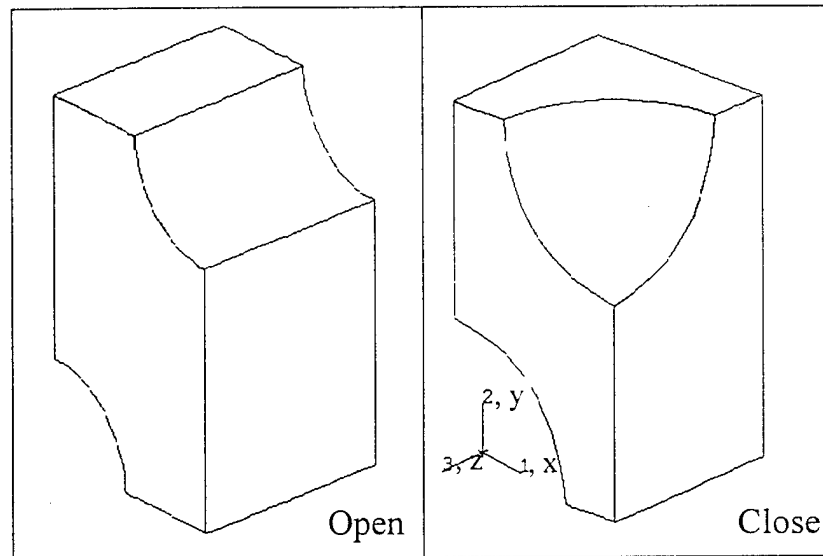

Figure 1. Unit cells for open pore and closed pore SMA material.

Assuming that the applied loads do not violate the geometric symmetry of the unit cell, one of the many possible representative unit cells, which can be used to predict the overall composite behavior, are given in Figure 1 for both open and closed pores. The boundary conditions for the unit cell in both cases are derived after taking into account both periodicity and symmetry conditions [13].

4. MESOSCALE REPRESENTATIVE VOLUME ELEMENT

Micromechanics examines the behavior of porous materials through the detailed evaluation of a single pore and the surrounding material. Limited pore interaction is included in micromechanical models. Mesoscale examines the behavior of porous materials through evaluation, in this case computational, of a volume containing multiple pores. Mesoscale modeling of a representative volume element (RVE) is used to determine pore interactions, pore spacing and pore size effects.
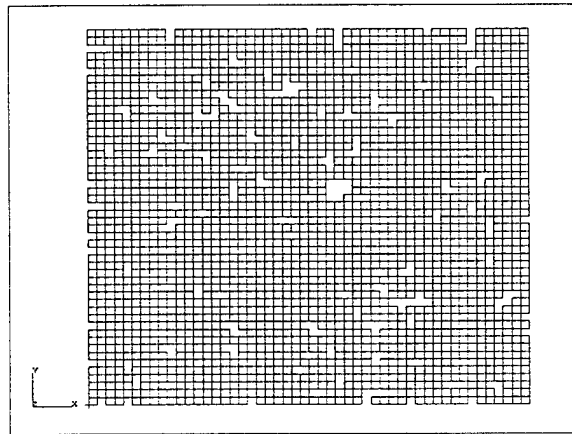

Figure 2. Finite element mesh of a 0.18 pore volume fraction randomly generated pattern.

A two-dimensional finite element mesh representative of a 1x1 mm region of porous SMA is generated. Uniform thickness of 1 mm is assumed. The mesh initially consists of 2500 equal-sized square four node linear solid elements in a 50 x 50 array. The porous microstructure is superimposed on this regular mesh by identification of elements that would be used to represent pores. Pores are placed in a random pattern. The unit pore is defined as a single element with a dimension of 0.02x0.02 mm. The volume represented by a unit pore is 0.0004 of the total RVE volume. Pores are placed randomly by matching integers associated with the random number sequence with element ID and are allowed to group with other pores. This allowed for generation of pores in the pattern that are larger than the unit pore enabling variations in pore shape. No limit is placed on the maximum pore size that could occur in the RVE. Figure 2 is representative of a 0.18 pore volume fraction pattern.

Two methods are used to model the material behavior of pores. For 0.18 pore volume fraction, pores are defined by removal of the identified elements. Then pores are represented by voids in the material. For higher porosity levels a very compliant material is used to define pores. This enables the generation of regions where material is completely surrounded by voided regions. This is a possible outcome of higher porosity in the two-dimensional representation. Use of a very

compliant material eliminated numerical instabilities associated with this isolation of material. The elastic modulus E_p used for pore material is defined as $10^{-9}E_{SMA}$. This value is determined by a sensitivity study of pore volume fractions of 0.18 and 0.33 and results in negligible differences in performance.

5. RESULTS AND DISCUSSION

The constitutive response of porous SMA is obtained for axial and transverse loading cases for both the unit cell finite element method and the Mori-Tanaka method. The effective response was obtained under each loading case for pore volume fractions ranging from 20% to 60% comparable to the experimentally observed values. The material parameters chosen for the analysis are presented in Table 1.

TABLE 1. SHAPE MEMORY ALLOY MATERIAL PARAMETERS

Material Parameters*	Values
E^A	70.0×10^9 Pa
E^M	30.0×10^9 Pa
$v^A = v^M$	0.33
$\rho\Delta c$	0.0 J/(m^3 K)
H	0.05
$\left(\dfrac{d\sigma}{dT}\right)^A = \left(\dfrac{d\sigma}{dT}\right)^M$	7.0×10^6 Pa/K
A^{of}	315.0 K
A^{os}	295.0 K
M^{os}	291.0 K
M^{of}	271.0 K
A - austenite, M - martensite *See references [10,11]	

The porous material is assumed to be initially stress-free and at the austenitic finish temperature A^{of}. The effective axial stress-strain response for the case of open pores is shown in Figure 3 for both the unit cell FEM and the Mori-Tanaka method for two different pore volume fractions: c_p=0.2 and c_p=0.6. For this particular loading, the only non-zero stress components are the axial components. Note in Figure 3 that the material initially behaves elastically with a distinct onset of the phase transformation. By the end of the loading, full phase transformation has taken place, and the material is in the martensitic phase. Upon unloading, a distinct start of reverse phase transformation takes place, and upon full unloading the material is in the austenitic phase, and all the strain is recovered. With increasing pore volume fraction, the critical applied stress required to initiate phase transformation in both forward and reverse phase transformation decreases. Also, softening of the material
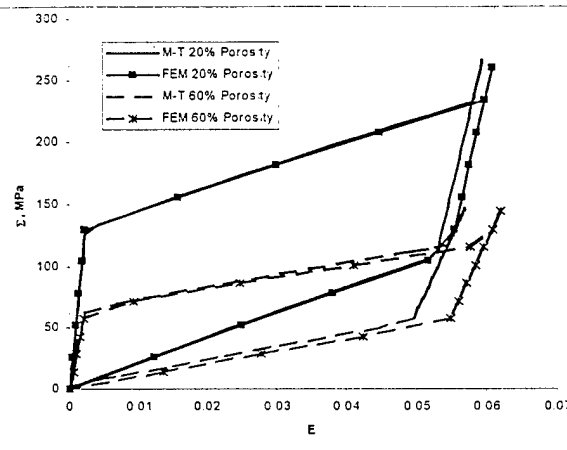
Figure 3. Comparison of effective axial stress-strain response of porous SMA for pore volume fractions of 0.2 and 0.6 as obtained by the unit cell FEM and the Mori-Tanaka method for the case of open porosity.

with increasing pore volume fraction occurs. It can be observed that for the case of 20% porosity (c_p=0.2), the results are in very good agreement. However, there is a discrepancy at the end of the phase transformation in the results for the case of 60% porosity (c_p=0.6).

The effective response under transverse loading for the case of open porosity is shown in Figure 4 for the same values of the pore volume fraction: c_p=0.2 and c_p=0.6. The transverse behavior is markedly different from the axial behavior. In the case of the unit cell FEM, the amount of the applied stress for each pore volume fraction is chosen such that the von Mises effective stress at any matrix material point does not become greater than 700 MPa. This value is chosen arbitrarily to mimic the yield stress of a dense SMA matrix, since stress-induced plasticity is not modeled presently. It is important to mention that near the pore the von Mises effective stress can be four to five times as high as the applied stress during phase transformation. Also, since the stress field in the matrix is inhomogeneous and
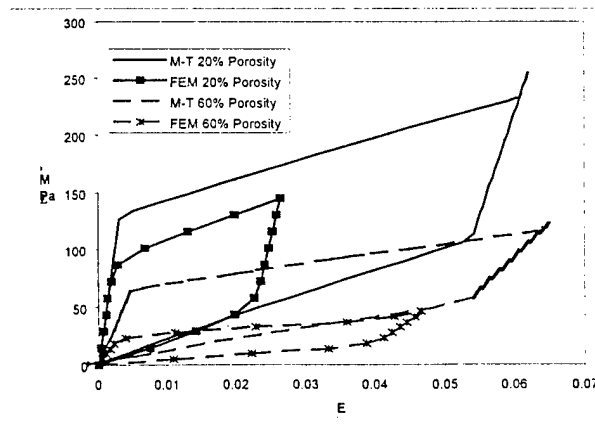

Figure 4. Comparison of transverse stress-strain response of porous SMA for pore volume fractions of 0.2 and 0.6 as obtained by the unit cell FEM and the Mori-Tanaka method for the case of open porosity.

increases non-proportionally during loading, phase transformation also occurs inhomogeneously throughout the matrix. In fact, as the FEM analysis showed, many regions of the matrix remain elastic until the end of loading depending on pore volume fraction. Consequently, unlike the axial case, the initiation of phase transformation is not distinctly obvious on the effective stress-strain curve. In addition, a decrease of critical applied stress for phase transformation and further softening of the material is observed as pore volume fraction increases (Figure 4).

Even though similar trends are observed in the results obtained by the Mori-Tanaka method, there is a significant difference in critical values of the applied stress and the maximum transformation strain. It can be observed that the critical value of the applied stress is much higher for the Mori-Tanaka method than for the unit cell FEM. This effect can be explained by recalling that due to stress concentration, the von Mises stress at material points near the boundary of the pore is approximately three times more than the applied stress during elastic loading, and at least four to five times more during phase transformation. Therefore, the transformation starts first at the points of stress concentration. However, the Mori-Tanaka method uses only the average value of stress, which of course is much smaller than the actual stress due to concentration. Thus, the onset of the phase transformation occurs much later for the Mori-Tanaka method than for the unit cell FEM. Another observation is that while the transformation does not take place throughout the matrix in the case of unit cell FEM, this is not the case if the Mori-Tanaka method is used since all material points in the RVE are assumed to behave in the same fashion. That is why transformation occurs uniformly throughout the matrix, and full transformation is obtained at a reasonable value of applied stress. The same value of applied stress would theoretically produce large plastic deformations at material points near the pore boundary in the periodic unit cell.

The comparison of the effective response for the case of closed porosity is shown in Figure 5 for pore volume fractions $c_p=0.2$ and $c_p=0.6$. It is observed that
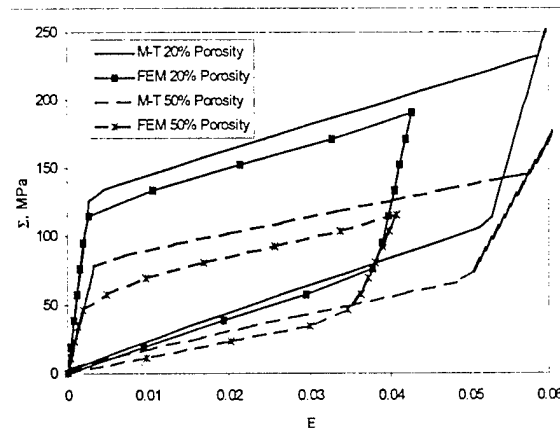

Figure 5. Comparison of effective stress-strain response of porous SMA for pore volume fractions of 0.2 and 0.6 as obtained by the unit cell fem and the Mori-Tanaka method for the case of closed porosity.

for the case of $c_p=0.2$ the onset of the transformation for both methods occurs at approximately 120 MPa, with little discrepancy observed. However, for the case of

c_p=0.6, substantial differences exist. Note that the difference between the two analyses is smaller compared to the open pore case. The reason is that even though stress concentration still exists near the pore boundaries, it is less severe for the spherical pores than for the cylindrical pores under transverse loading. Thus the difference between the averaged stress concentration calculated by the Mori-Tanaka method and the local stress concentration demonstrated by the unit cell FEM is decreased.

Next the mesoscale finite element analysis results for c_p=0.2 are presented. The global stress-strain response in the x-direction is shown in Figure 6 for mesoscale and unit cell analyses. The effective response was obtained by applying uniform displacement boundary conditions along one edge of the RVE, while constraining motion in the loading direction along the opposing edge. The RVE is free to contract in the other direction. As seen in Figure 6, the material behaves elastically under initial loading and then smoothly begins to exhibit phase transformation. The smooth transition is the result of the non-uniform effective stress field within the RVE. The unloading begins when an arbitrary value of strain concentration factor[1] is reached at any material point inside the RVE. Limited phase transformation occurs throughout the region until that moment (not shown here). Upon unloading, reverse phase transformation again takes place smoothly and full recovery of the material takes place as expected.
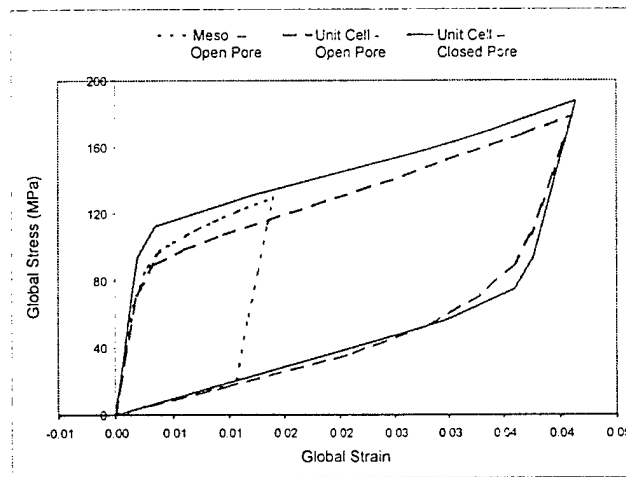

Figure 6. Comparison of global stress-strain response of porous SMA in the x-direction for mesoscale and unit cell FEM analyses.

The amount of effective applied stress required to induce phase transformation as predicted by the mesoscale analysis falls within the bounds of open pore and

---

[1] The strain concentration factor is defined as $\frac{\varepsilon_{max}}{\varepsilon_{app}}$, where ε_{max} is the maximum strain in the direction of applied load and ε_{app} is the applied strain.

closed pore unit cell analyses. Phase transformation hardening rates are also similar. However, it is also noted that to achieve similar levels of transformation as obtained for the unit cell analysis, a higher applied strain is required, which will result in severe deformation at many material points. Such an analysis may not be physically realistic without taking into account dislocation based plasticity.

6. CONCLUSIONS

The macroscopic response of porous SMAs is studied using micromechanical techniques by treating the porous SMA as a composite made of a dense SMA matrix with a distribution of pores. The unit cell FEM is employed to determine the effective behavior for a periodic distribution of pores, and the Mori-Tanaka averaging method is employed to determine the effective mechanical behavior for a random distribution of pores under isothermal conditions. In addition to these two methods, a mesoscale model of porous SMA is also presented. All methods show similar variation of elastic constants with respect to the pore volume fraction. The effective stress-strain response during phase transformation as obtained by the Mori-Tanaka method and the unit cell FEM is in good agreement for the case of axial loading of open-pore porous SMA. The discrepancy observed for the other loading cases is attributed to the averaging scheme applied in the Mori-Tanaka method that smoothes the stress concentration. Reasonable agreement is achieved for low to moderate (0.26 and lower) levels of pore volume fraction between the unit cell FEM and the mesoscale results. At the pore volume fraction of 0.33, results from the two computational methods diverge.

To make a comparison with the experimental data, recall Figures 5 and 6 from Part I. The slope during the elastic loading (the material is in austenite) for the results presented in Figure 5 is approximately 16 GPa, while the slope at the beginning of the unloading (the material is in martensite) is approximately 11 GPa. The Mori-Tanaka approximation of these two parameters is 26 GPa and 11 GPa, respectively. Thus the approximation of the elastic modulus is in good agreement for the martensite phase, while some discrepancies are observed for the austenite phase. However, as seen in Figure 5 of Part I, the material response is non-linear form the beginning of the test, which indicates the start of the martensitic transformation. Thus, it is concluded that the stiffness is reduced which explains the observed discrepancy.

The slope at the beginning of the unloading (see Figure 6, Part I) is approximately 20 GPa, which again disagrees with the Mori-Tanaka approximation. However, there is evidence that the material may not be fully transformed at the beginning of the unloading, i.e., part of the material is still in the austenite (stiffer) phase. This untransformed material is responsible for the overall stiffer response.

REFERENCES

1. L.J. Gibson and M.F. Ashby, *Cellular Solids: Structures and Properties, 2nd ed.* Cambridge University Press, Cambridge 1999.
2. C.T. Herakovich, and S.C. Baxter, "Influence of pore geometry on the effective response of porous media", *Journal of Material Science* **34**, pp.1595-1609, 1999.
3. S. Breuer and S. Jägering, "Numerical calculation of the elastic and plastic behavior of saturated porous media", *International Journal of Solids and Structures* **36**(31-32), pp.4821-4840, 1999.
4. R.J. Green, "A plasticity theory for porous solids", *Int. J. mech. Sci.* **14**, pp. 215-224, 1972.
5. A.L. Gurson, "Continuum theory of dictile rupture by void nucleation and growth: Part I - Yield criteria and flow rules for porous ductile media", *Journal of Engineering Materials and Technology* **99**, pp.2-15, 1977.
6. H.-Y. Jeong and J. Pan, "A macroscopic constitutive law for porous solids with pressure-sensitive matrices and its implications to plastic flow localization", *International Journal of Solids and Structures* **32**(24), pp.3669-3691, 1995.
7. D.C. Lagoudas, A.C. Gavazzi, and H. Nigam, "Elastoplastic behavior of metal matrix composites based on incremental plasticity and the Mori-Tanaka averaging scheme", *Computational Mechanics* **8**(3), pp. 193-204, 1991.
8. D.C. Lagoudas, J.G. Boyd and Z. Bo, "Micromechanics of Active Composites with SMA Fibers", *Journal of Engineering Materials and Technology* **116**, pp.337-347, 1994.
9. M. Cherkaoui, Q.P. Sun and G.Q. Song, "Micromechanics modeling of composite with ductile matrix and shape memory alloy reinforcement", *International Journal of Solids and Structures* **37**, pp. 1577-1594, 2000.
10. D.C. Lagoudas, Z. Bo, and M.A. Qidwai, "A unified thermodynamic constitutive model for SMA and finite element analysis of active metal matrix composite", *Mechanics of Composite Materials and Structures* **3**, pp. 153-179, 1996.
11. M.A. Qidwai, and D.C. Lagoudas, "Numerical implementation of a shape memory alloy thermomechanical constitutive model using return mapping algorithms", *International Journal of Numerical Methods in Engineering* **47**, pp. 1123-1168, 2000.
12. A.C. Gavazzi and D.C. Lagoudas, "On the Numerical Evaluation of Eshelby's Tensor and its Application to Elastoplastic Fibrous Composites", *Computational Mechanics* **7**, pp. 13-19, 1990.
13. D.C. Lagoudas, P.B Entchev, M.A. Qidwai and V. DeGiorgi, "Modeling of Porous Shape Memory Alloy Behavior", In: Smart Materials and Structures 2000, SPIE. In press.